PRELIMINARY GEOLOGIC DESCRIPTION

S. A. HOLDITCH & ASSOCIATES
SFE NO. 2

November, 1987

Prepared by

Shirley P. Dutton, Robert S. Tye, Stephen A. Laubach,
Karen L. Herrington, and James Miller

Bureau of Economic Geology
W. L. Fisher, Director
The University of Texas at Austin
Austin, Texas 78713-7508

Prepared for

The Gas Research Institute
Contract No. 5082-211-0708
Robert J. Finley and Shirley P. Dutton,
Co-principal Investigators

INTRODUCTION

Four intervals of the Travis Peak Formation were cored in the S. A. Holditch & Associates SFE No. 2 well, North Appleby field, Nacogdoches County, Texas. Core was recovered from 8,230.0 to 8,319.7 ft, 8,678.2 to 8,738.0 ft, 9,480.0 to 9,572.1 ft, and 9,806.7 to 9,942.1 ft. The top of the Travis Peak is at 8,000 ft (log depth), so the core samples are from 230 ft to 1,942 ft below the top of the formation.

MACROSCOPIC CORE DESCRIPTION

Macroscopic sedimentary characteristics of cores representing four stratigraphic intervals from 8,230.0-8,319.5 ft (cores 1-3); 8,678.0-8,738.0 ft (cores 4 & 5); 9,480.0-9,572.2 ft (cores 6-8); and 9,806.5-9,942.0 ft (cores 9-15) from the SFE No. 2 well were logged using standard sedimentologic techniques. A hand lens and binocular microscope were used to provide a visual estimate of the range in sediment grain sizes present. The vertical scale at which the cores were logged is 1 inch = 5 ft. Primary characteristics noted on the logging form (see appendix) included: 1) lithology (rock type); 2) sedimentary structures (primary and biogenic); 3) sediment grain size; and 4) texture (sorting). Secondary attributes also included in the descriptions are: 1) induration; 2) relative occurrence of $CaCO_3$ cement; 3) color; 4)bedding contacts (scoured, sharp, gradational, broken, etc.) and 5) accessories (bitumen, organic material, diagenetic nodules). Core depths were adjusted to log depths using a best-fit technique of correlating the down-hole gamma-ray log with a core-gamma log run at the Bureau of Economic Geology.

Five lithofacies are defined in the fifteen cores, and based on their sedimentary character, they are interpreted to represent discrete depositional environments. The lithofacies are: 1) crossbedded and rippled medium-to fine-grained sandstone with thin clay-clast conglomerate layers (channel); 2) interbedded rippled very fine- to fine-grained sandstone and burrowed silty sandstone (abandoned channel); 3) laminated to burrowed sandy mudstones (lacustrine); 4) rooted and burrowed silty sandstones and sandy mudstones (floodplain); and 5) rippled to burrowed silty sandstones (floodplain sandstones). The floodplain sequences contain sandstones and silty sandstones that are interpreted to be crevasse splay or lacustrine delta deposits. Presently, this distinction cannot be made, therefore these sediments are referred to as floodplain sandstones.

Interpretations for the depositional history of the four stratigraphic intervals cored in the Travis Peak are preliminary. Environmental interpretations are subject to change pending further research currently in progress, such as: 1) constructing detailed stratigraphic correlations between all wells in North Appleby field; 2) combining interpretations from cores in SFE No. 2 with information from cores in the Prairie Mast No. 1-A well; and 3) mapping individual stratigraphic units to determine geometries and sand content.

Sedimentology

Sediments in all fifteen cores from SFE No. 2 are interpreted to have been deposited in depositional environments associated with major fluvial systems (active and abandoned channel, lacustrine, and floodplain) that evolved during Travis Peak deposition. Previous core studies have interpreted much of the Travis Peak sediments as having been deposited in high bed-load, broad, braided streams (Dutton, 1987). Cores from SFE No. 2 indicate that these fluvial systems evolved

through time, changing from broad low-sinuosity sand-rich channels during early deposition (model 9; Miall, 1985) to relatively deeper low-sinousity channels (model 10; Miall, 1985) later.

Brief descriptions of each depositional environment are given below, and the vertical arrangement and interpretation of each cored interval follows. Cored intervals are described in ascending order.

Lithofacies 1 and 2 (Channel and Abandoned Channel)

Channel sandstones are generally very fine-to fine grained, have scoured bases, and commonly exhibit internal scour contacts. Channels in the lowermost cored interval are the coarsest-grained (fine- to medium-grained). Channel sandstones may include clay-clast conglomerates with clast size ranging up to pebbles. The primary bedding type in the basal portion of the channels is planar cross-bedding (sets average 0.3 ft thick), which grades upward into thinly interbedded sets of planar crossbeds and rippled beds. Other features of these sandstones include massive-appearing beds, beds of horizontal to gently inclined laminae, detrital organics concentrated on bedding surfaces, and abundant ripped-up mud clasts.

Thicknesses of channel deposits vary in the four cored interals. Channels range from 30 to 50 ft thick and are best-developed in the lowermost interval (cores 9-15). Vertical thickness of channel deposits is often increased by the stacking of separate channel bodies. This is particularly evident in the shallower intervals (cores 6-8 and 1-3). On gamma-ray logs, channel sandstones have blocky to irregular log patterns. Channel bases are generally sharp, but the gamma-ray log underestimates the actual channel thickness because clay-clast lags (clast size up to 0.12 ft) on the channel bases are seen as "shales". Many "shaley" breaks

noted by the log are actually channel-lag deposits, and stacking of these channel deposits gives the log patterns of the sandstones an irregular appearance.

Abandoned channel deposits abruptly to gradationally overlie the channel sandstones and are represented on the gamma-ray log by an overall upward-fining serrate pattern. In core, these deposits consist of thin- to medium-bedded fine- to very fine-grained sandstone, silty sandstone, and mudstone. The prevailing conditions of low sediment input and weak depositional energies in the abandoned channels are reflected in the increased mud content of the sediments and the greater activity of burrowing organisms. Trough and planar ripple cross-laminations are common, and ripple foresets are often accentuated by flaser beds and organic drapes. Pyrite associated with the detrital organics is abundant. Beds up to 1.5 ft thick contorted by soft-sediment deformation occur within the abandoned channel deposits. Burrows and occasional rooting structures have obliterated primary structures in the uppermost portion of the abandoned channel sequences.

Lithofacies 3 (Lacustrine)

Lacustrine sequences are thin (<6.0 ft) and not abundant in the cored intervals. They consist of intensely burrowed to occasionally laminated and rippled sandy siltstones to silty sandstones. Burrowing is the dominant feature, but lacustrine sediments may also be rooted. Some organic matter is preserved.

Lacustrine deposits overlie floodplain sediments and are commonly overlain by a coarsening- or fining-upward muddy sandstone. This association imparts an upward-fining, shaly character to the lacustrine deposits on the gamma-ray log, but as the lacustrine deposits are overlain by sandstones, a sharp upper contact is often noted.

Lithofacies 4 (Floodplain)

Densely rooted and burrowed, red to greenish-grey and black sandy mudstones represent the floodplain environment. The thickness of cored floodplain sequences ranges form 2 to 15 ft. Intense biogenic reworking gives these deposits a mottled appearance, and, rarely, primary sedimentary structures such as laminations or ripples are preserved.

Disseminated organic matter in the form of "coffee grounds" is common in the floodplain sediments, as are diagenetic carbonate nodules. Pyrite is absent, therefore it is believed that these floodplains were fairly well drained.

Floodplain deposits exhibit serrate to uniform "shaley" patterns on the gamma-ray log. More thickly developed floodplains have a serrate appearance on the lithologic log due to the inclusion of thin, mud-rich sandstones.

Lithofacies 5 (Floodplain sandstones)

Thin (4 to 12 ft), muddy, fine- to very fine-grained sandstones commonly overlie or are interbedded with floodplain and lacustrine deposits. These sandstones can form both coarsening- and fining-upward sequences. As these sandstones are interpreted to have been deposited by traction processes during flood events, but later reworked by biogenic processes on the floodplain, their internal stratification can be extremely complex.

Planar crossbeds, planar and trough ripple laminations, and distorted beds (slumps and dewatering structures) are the most abundant physical structures. Normally graded and reverse-graded beds (0.5 to 3.0 ft thick) are common. Depending on the intensity of the physical processes and the rate of burial, organisms can burrow through the entire sequence and destroy primary

stratification. Rooting is apparent at the top of some floodplain sandstones. Most floodplain sandstones appear as sharp-based and sharp-topped beds on the gamma-ray log.

Interpretation of Cored Intervals

Cores 9-15

The gamma-ray log character between 9,802.0 and 9,947.0 ft (log depth) implies the presence of three stacked, upward-fining sandstones (fig. 1) in the lower Travis Peak Formation (approximately 190 ft above the Cotton Valley). As indicated by the serrate gamma-ray log signature, the sharp-based blocky sandstones are separated vertically by thickly bedded (2.0 ft) muddy sandstones and mudstones. In the corresponding cored intervals, beds of clean sandstone vary in thickness from 0.5 to 21.0 feet whereas muddy sandstones and mudstones range from laminations 0.01 ft thick to beds up to 23.0 ft thick. Core to log correlations are informative in that "shaley" intervals as indicated by the SP and gamma-ray logs are actually silty sandstones to sandy mudstones. No true shale is present in this lower cored interval.

Vertical lithologic associations and sedimentary characteristics revealed in cores 9-15 suggest that the three thick sandstones are fluvial in origin. Sandstones and mudstones deposited in abandoned channel and floodplain swamp environments vertically separate these fluvial channels. Thin mud-breaks in the channel sands represent blocks of floodplain sediments slumped into the channels and poorly developed abandoned channel deposits. A well-developed, organic-rich, rooted and burrowed mudstone (9896 to 9911 ft, log depth), interpreted as being a floodplain

swamp, separates channels 1 and 2 (fig. 1). Incipient floodplain soils developed between other channels at the top of abandoned channel-fill deposits.

Cores 6-8

Blocky to irregular, coarsening to fining-upward sandstones occurring between the intervals of 9,484 to 9,528 ft and 9,532 to 9,570 ft (log depth) account for most of the sedimentary sequence in cores 6-8 (fig. 2). The gamma-ray log indicates that these sandstones, which average 10 ft thick, are separated by thin (2 to 5 ft) mudstone beds, and the multiple occurrence of these "muddy breaks" gives this interval an erratic log response. Core descriptions reveal that although some mudstone beds do separate the sands, many of the breaks are caused by the inclusion of ripped-up mud clasts in the sandstones.

The sandstones are interpreted to have been deposited in shallow, poorly developed channels that were stacked vertically. The basal portion of core 8 and the top of core 7 recovered thin floodplain and floodplain-sandstone deposits that separate the channels (fig. 2). That multiple channels are stacked is evidenced in the core by scoured contacts of sandstone into sandstone, some of which are highlighted by mud-clast conglomerates.

Cores 4-5

Cores 4 and 5 recovered interbedded sandstone and mudstone from 8,676 to 8,738 ft (log depth). The sandstones are variable in thickness (2 to 28 ft), are thin and interbedded with mudstone near the base, and form a thick, fining-upward deposit above. Intervening mudstones are 2 to 6 ft thick, and result in a serrate gamma-ray log pattern.

The interbedded mudstones and sandstones in the lower portion of core 5 are floodplain and floodplain-sandstone deposits. The sandstones exhibit sharp bases, have basal mud-clast lags, and fine-upward (fig. 3). Mudstones separating them are rooted and burrowed and contain plant debris.

A fining-upward sandstone that occurs near the top of core 5 and continues into core 4 was deposited in a fluvial channel. The sandstone is planar crossbedded, rippled, and horizontally laminated. It grades upward into burrowed and contorted silty sandstone of the abandoned channel-fill.

Cores 1-3

The stratigraphic interval represented by cores 1-3 (8,229 to 8,259 ft and 8,266 to 8,322.5 ft, log depth) consists of basal interbedded sandstones and mudstones that overlie a thick (27 ft) sandstone, and are abruptly overlain by two stacked sandstones that have a combined thickness of 42 ft. Sandstones are variable in thickness (5 to 18 ft), but they thicken upward. Mudstones are from 4 to 9 ft thick. Significant "shale" breaks noted by the gamma-ray log at 8,254 and 8,280 ft are actually layers of ripped-up mud clasts with thicknesses of 0.5 and 2.0 ft, respectively.

Core 3 penetrates the upper portion of a 27-ft thick channel deposit that is separated from channel sandstones in cores 1 and 2 by 35 feet of mudstones and sandstones representing abandoned-channel, lacustrine, and floodplain environments (fig. 4). Sediments in this fine-grained interval are densely burrowed, commonly rooted, organic-rich, and occasionally rippled to laminated. Channels scoured into the floodplain mudstones, and the scour contacts are draped by ripped-up mud clasts. Channel sandstones are dominantly planar crossbedded, horizontally

laminated, and rippled. Some soft-sediment deformation is apparent. Rooted red and grey floodplain mudstones cap the channel deposits.

PETROGRAPHIC DESCRIPTION

Detailed study of the core is being conducted with a standard petrographic microscope and with a scanning electron microscope (SEM) that includes an energy dispersive X-ray system (EDX).

Grain Size

Analysis of grain size was accomplished by making grain-size point counts of thin sections. Fifty grains per slide were measured along their long dimensions, excluding cement overgrowths, in order to determine the size of the detrital grains. Mean diameter of sand- and silt-sized grains was calculated for each sample (table 1); detrital and authigenic clays were not included in the calculation of mean grain diameter.

All sandstone samples in the Holditch SFE No. 2 well are fine or very fine grained (0.06 to 0.25 mm). Most silt is coarse silt, between 0.031 and 0.063 mm, and clay particles are smaller than 0.004 mm. The samples are classified texturally as sandstone, silty sandstone, and muddy sandstone (table 1).

Mineral Composition

Thirteen thin sections have been point counted for a preliminary description of mineral composition in SFE No. 2 sandstones (table 2). The sandstones are

mineralogically mature and are classified as quartzarenite to subarkose. Quartz comprises 78% to 98% of the essential framework constituents (quartz, feldspar, and rock fragments). Plagioclase is generally more abundant than orthoclase, and total feldspar volume varies from 0% to 19%. Orthoclase occurs in the deepest samples (table 2), considerably lower in the Travis Peak Formation than it has been seen in other cores. The reason why orthoclase was not dissolved is not known. Rock fragments, mainly chert and low-rank metamorphic rock fragments, constitute between 0% and 4% of the framework grains.

Authigenic cements and replacive minerals constitute between 23% and 59% of the rock volume in these 13 samples (table 2). Authigenic quartz, illite, chlorite, kaolinite, dolomite, ankerite, anhydrite, feldspar, pyrite, and reservoir bitumen have all been observed in Holditch SFE No. 2 thin sections. The sample with a total of 59% authigenic minerals contains abundant ankerite cement and nodules that replace framework grains and detrital clay matrix.

Quartz cement is the most abundant authigenic mineral in most samples (table 2). Quartz overgrowths fill as much as 29% of the sandstone volume, and precipitation of authigenic quartz occluded much of the primary porosity (fig. 5). Quartz cement also lines many fractures (fig. 6), as discussed in more detail in the section on natural fractures. Sandstones that lack detrital clay matrix contain an average volume of 23.5% quartz cement, which is higher than the overall average for clean Travis Peak sandstones in East Texas (Dutton, 1987).

Authigenic illite and chlorite occur most commonly as pore-filling cements in secondary pores that formed by dissolution of feldspars. Illite also occurs as thin, tangentially-oriented rims around detrital grains. Authigenic clays in secondary pores formed relatively late in the burial history of the Travis Peak after precipitation of quartz cement.

SEM analysis of the effect of air-drying on illite morphology was conducted on samples from the Holditch SFE No. 2. Samples were taken by plugging into the center of the core where there was the least probability of the core having dried out. A pair of chips were taken from each plug; one was air-dried, and the other was flash frozen in liquid nitrogen and then freeze-dried under vacuum. SEM analysis showed that air-drying drastically alters illite morphology. The freeze-dried samples contained abundant illite present as long, delicate thin fibers (fig. 7). In the air-dried samples, the fibers had either matted together forming thicker "ropes" of illite or else completely collapsed and plated out against the walls of the pores (fig. 8). This change in illite morphology upon air drying could also occur in plugs used for routine core analysis, and it may significantly increase measured permeability.

Dolomite and ankerite occur as pore-filling cements and as replacive minerals. Dolomite ranges in volume from 0% to 1.5% in the samples from the two upper cored intervals but is absent in the lower Travis Peak cores. In general ankerite is more abundant in upper Travis Peak samples, but two samples from the lower Travis Peak, at 9,543 and 9,838 ft, contain 27% to 56% ankerite (table 2). Abundant ankerite cement could cause completion problems (formation of iron-hydroxide gel) if it is treated with acid.

The ankerite in the sample from 9,838 ft is distributed evenly throughout the sandstone, but it appears to occur preferentially between grain boundaries, commonly replacing earlier quartz cement. Its distribution suggests permeability pathways remained open between crystal faces of quartz overgrowths. Thus, the ankerite provides evidence that fluid movement through intercrystalline porosity continued even after the extensive quartz cementation; late-stage fluid movement was not confined to fracture porosity.

Minor amounts of anhydrite cement were observed in a sample from 9,909.6 ft (table 2). The anhydrite is a late, diagenetic feature and did not precipitate in the depositional environment.

Reservoir bitumen is most abundant in the upper part of the core, but it is present as deep as 9,889 ft. In other Travis Peak cores, reservoir bitumen is rare more than about 300 ft below the top of the Travis Peak. The nearby Prairie Mast No. 1-A core had no reservoir bitumen deeper than 9,212 ft.

Porosity

Porosity observed in thin section varies from 0% to 6.0% (table 2), considerably lower than thin section porosity in SFE No. 1. Both primary and secondary pores are present. Secondary pores are formed by the dissolution of framework grains, so they are approximately the same size as detrital grains. Secondary pores are commonly partially filled by authigenic clays and remnants of detrital feldspar. Porosity measured by point counting thin sections is usually lower than porosity measured by porosimeter on adjacent samples because of the presence of abundant microporosity. Microporosity occurs in detrital and authigenic clays; such porosity generally cannot be seen in thin section, but it can be observed by SEM and is measured by porosimeter.

NATURAL FRACTURES

Preliminary observations of SFE No. 2 core show that natural fractures in Travis Peak sandstone are a potential hydrocarbon reservoir and a potential influence on hydraulic fracture treatment. Fractures are common in low permeability Travis Peak sandstone, and fractures that were open in the subsurface were recovered from a range of depths including depths of greater than 9,900 ft. Some open fractures have widths exceeding 4 mm (fig. 9) although most are narrower (table 3). Hydrocarbon fluorescence was observed on some fracture surfaces, and mud gas shows occurred in some fractured intervals, suggesting that these natural fractures contain hydrocarbons. Fractures created in naturally fractured intervals during stress tests have multiple intersecting fracture strands that may indicate how natural fractures influence the geometry of engineered hydraulic fractures.

Preliminary field descriptions of fractures were made by BEG and CER. Fractures were described in the field using a handlens. Detailed study of fractures using binocular, petrographic, and scanning electron microscopes is in progress. Fractures were interpreted to be either natural or coring-induced on basis of the criteria of Kulander and others (1979). Fracture orientation is being determined from borehole televiewer (BHTV) logs supplemented and checked by paleomagnetic core orientation in selected intervals. Preliminary fracture orientations were obtained from field prints of the Schlumberger BHTV log. Below, some of the salient characteristics of natural extension fractures in SFE No. 2 core are summarized since these fractures could potentially affect hydraulic fracture treatment and reservoir characteristics.

Fracture Type

A total of 169 fractures are present in the core, of which 48 are natural and 121 are the result of drilling, coring, or stress tests. Natural fractures can be divided into two types: (1) mineralized extension fractures and (2) striated shear fractures. Mineralized extension fractures occur predominantly in sandstone, whereas striated shear fractures are restricted to muddy siltstone and mudstone. Forty extension fractures (table 3) and eight shear fractures were cored. Extension fractures are more common than shear fractures in SFE No. 2 core because the core is approximately 80% sandstone.

Fracture abundance or intensity is difficult to quantify with vertical core in the Travis Peak because fracture dip is subparallel to the core axis, and fracture spacing is generally greater than the four-inch diameter of the core, implying a fracture spacing of greater than 10 cm. One qualitative measure of fracture abundance that accounts for the dependence of fracture occurrence on rock type is the fracture number, defined as the total length of fractures in core normalized to the thickness of cored sandstone. On the basis of the fracture number, natural fractures are more abundant in SFE No. 2 than in GRI Travis Peak wells in Harrison County (Laubach and others, 1987), and fractures are more abundant in the lower part of the Travis Peak than in the upper part in SFE No. 2 (fig. 10). Greater fracture intensity with depth in SFE No. 2 is also suggested by the local occurrence in the lower Travis Peak of parallel fractures with spacing of only 4 to 5 centimeters (fig. 9).

Fracture Orientation

Fracture strike in oriented core is east-west, consistent with the strike of fractures observed on BHTV logs (fig. 11). Fracture dip is generally steep, usually

within 10 degrees of vertical. Locally, subhorizontal fractures intersect subvertical fractures, but petrographic study is required to determine if these subhorizontal fractures are natural. Where several subvertical, inclined fractures occur in the same core, the fractures generally dip in the same direction and do not intersect. The opposed dips of fractures 8/5 and 8/6, which intersect at 9,847 ft, is a notable exception. Fracture zones composed of closely spaced, parallel fracture segments were noted on the preliminary field description (table 3). Individual segments of these fracture zones are not necessarily in contact with one another. In cross section, fracture segments are commonly arranged in en echelon or relay patterns, and the fracture pattern in map view is probably similar. Locally, arrays of parallel fractures or more complex patterns are present (fig. 9a). Across-strike connectivity of fractures is probably poor. Despite the common occurrence of orthogonal fracture patterns in rocks at the earth's surface, examination of SFE No. 2 core and BHTV and core collected from previous GRI wells shows no evidence of a second fracture set at a high angle to the east-trending set.

Fractures and interconnected fracture zones range in length from a few inches to over ten feet (fracture 13/8 at 9,870-9,880.3) (table 3). The average length of fractures in core is 1.5 ft, but this is an underestimate because many fractures that do not terminate within the core are included in the average. Fracture width ranges from less than 0.05 mm to 5 mm, with an average width of 0.7 mm. The widest fractures occur in the deepest cored intervals (table 3). In cross section, fractures are lens-shaped (ellipses) with a wide range of length to width ratios (table 3). Tall, narrow fractures are most common, but short, wide fractures provide examples of vug-like porosity. Commonly, fractures have simple, gradually tapering terminations, but branching and blunt terminations are also present. Simple, tapering terminations occur at both mudstone interbeds and within apparently homogeneous sandstone.

Minerals in natural fractures include quartz, minor carbonate, minor anhydrite, and clay minerals. Quartz occurs on all natural extension fracture surfaces as a veneer usually less than 0.12 mm thick. Preliminary SEM observations suggest that this quartz layer may not isolate fractures from intergranular porosity. Locally, the quartz veneer is overgrown by acicular quartz crystals oriented normal to the fracture face (figs. 6 and 9). Fractures with faceted quartz crystals on opposed fracture faces were open in the subsurface (fig. 6). Carbonate minerals and anhydrite are less abundant than quartz and are absent in many fractures (table 3). Carbonate and anhydrite mineralization followed quartz precipitation, and preliminary observations suggest anhydrite was precipitated after carbonate minerals in the fractures.

Three open-hole stress tests were carried out during the coring, and fractures created in the stress tests were cored. Fractures created during stress tests were recovered from below stress tests 2 and 3; fractures in core below stress test interval 1 are still being studied to determine if they were created in the stress test or not. In stress tests 2 and 3, more than ten individual fracture planes created by the stress test were recognized. Fractures below stress test interval 2 (Core 7) include at least three long fracture planes (fig. 12). These fractures contrast with the simple, planar fractures recovered from stress test intervals in the Holditch Howell No. 5 (CER Corporation, 1987). Stress tests 2 and 3 are in intervals containing natural fractures.

Table 1. Grain-size distribution in Holditch SFE No. 2 cores.

Depth (ft)	Mean (mm)	Sand (%)	Silt (%)	Detrital clay (%)	Authigenic clay (%)	Textural class
8270.5	.114	86.9	7.6	0	5.5	Sandstone
8275.5	.104	86.9	9.7	1.4	2.0	Silty sandstone
8700.8	.112	92.6	3.9	0	3.5	Sandstone
8711.9	.098	75.6	14.4	10.0	0	Muddy sandstone
8714.0	.100	81.3	13.2	1.0	4.5	Silty sandstone
8731.5	.105	63.6	17.9	1.8	0.5	Muddy sandstone
9490.7	.181	97.0	0	0	3.0	Sandstone
9530.0	.182	95.0	0	0	5.0	Sandstone
9543.0	.211	90.2	7.8	2.0	0	Sandstone
9811.0	.157	95.5	0	0	4.5	Sandstone
9838.0	.243	98.5	0	0	1.5	Sandstone
9909.0	.087	79.5	13.0	2.0	5.5	Silty sandstone
9930.0	.166	91.7	5.8	0	2.5	Sandstone

Table 2. Petrographic analyses of Holditch SFE No. 2 core.

	Framework grains								Matrix
Depth (ft)	Quartz	Plagioclase	Orthoclase	MRF	Chert	Clay clasts	Mica	Other	Clay-sized fines
8270.5	51.0	5.0	2.5	0	1.0	5.0	0	1.0[1,2]	0
8275.5	54.5	5.0	2.0	0	0	6.0	0	1.0[2,3]	1.5
8700.8	51.5	6.0	2.5	0	0	2.0	0	0.5[4]	0
8711.9	48.5	2.0	2.5	0.5	0	4.5	0.5	0.5[3]	10.0
8714.0	45.0	4.0	7.0	0	1.0	6.0	0	1.0[3]	1.0
8731.5	50.5	1.5	3.5	1.0	0	1.0	1.0	0	18.0
9490.7	61.0	1.0	0.5	0	1.0	0.5	0.5	0.5[3]	0
9530.0	63.0	3.5	3.5	1.0	1.0	3.5	0	0.5[4]	0
9543.0	36.0	0	1.0	0.5	0	1.0	0	0.5[4]	2.0
9811.0	62.0	0.5	0	0	1.0	2.0	0	0	0
9838.0	54.5	0	0	0.5	0.5	1.0	0	0.5[5]	0
9909.6	51.0	2.5	2.0	0	0.5	8.5	0	2.5[1,4,6]	2.0
9930.0	63.0	2.0	0.5	0	1.5	0.5	0	0	0

[1] Kaolinite cement

[2] Reservoir bitumen

[3] Zircon

[4] Wood fragment

[5] Tourmaline

[6] Anhydrite cement

Table 2 (cont.)

Depth (ft)	Cements							Porosity	
	Quartz	Dolomite	Ankerite	Illite	Chlorite	Pyrite	Feldspar	Primary	Secondary
8270.5	25.0	0.5	2.0	4.5	0.5	0	0.5	0	1.5
8275.5	22.0	1.0	3.5	2.0	0	0.5	0	0	1.0
8700.8	29.0	1.5	3.0	3.5	0	0	0	0	0.5
8711.9	12.5	1.0	14.0	0	0	1.0	0.5	0	2.0
8714.0	21.5	0.5	6.5	4.5	0	0.5	0	0	1.5
8731.5	11.0	1.5	9.0	0	0.5	0.5	0	0	1.0
9490.7	28.5	0	0	3.0	0	0	0	2.5	0.5
9530.0	17.0	0	0.5	5.0	0	0	0.5	0.5	0.5
9543.0	3.0	0	55.5	0	0	0	0.5	0	0
9811.0	29.0	0	0	4.5	0	0	0	0	1.0
9838.0	8.5	0	27.0	1.5	0	0	0	2.5	3.5
9909.6	24.5	0	0	5.0	0	1.5	0	0	0
9930.0	27.5	0	0	2.5	0	0	0	0	2.5

Table 3. Natural Extension Fractures in Holditch SFE No. 2 Core.

Core No.-Fracture No.	Core Depth (ft)	Width (W) (mm)	Length (L) (mm)	$\frac{L}{W}$	Rock Type	Vein Minerals	Notes
1-11	8251.4-8252.0	0.31	182	587	ss	Q+cc	4,5
2-1	8266.3-8267.8	0.55	457		ss	Q+cc?	1,2,5,6
2-3	8272.1-8272.6	0.05	61		ss	Q	1
2-4	8276.0-8276.4	0.05	122	2,440	ss	Q	2,4
6-4	9481.4-9486.4	--			ss	--	3,5,7
6-5	9486.6-9490.3	1.10	1,128		ss	Q	1,2,4,5
6-7	9491.8-9492.7	0.05	274		ss	Q	3,4
6-10	9497.4-9501.5	0.80	1,250		ss	Q	1
7-1	9510.1-9514.2	0.50			ss	Q?	1,6
7-5	9512.1-9514.9	--			ss	--	3,6,7
7-12	9525.2-9526.9	--	427		ss	Q?	
7-15	9533.4-9534.0	<0.05	183		ss	Q	3
8-5	9546.8-9548.7	0.84	579		ss	Q+Anhy	3,5
8-6	9548.1-9549.1	0.84	30		ss	Q+Anhy	1,5
8-7	9549.7-9550.4	0.05	213		ss	Q	2,5
8-10	9554.5-9555.1	1.20	183	152	ss	Q?	4,5
8-13	9560.8-9562.9	0.05	64		ss	Q+cc	3,4,5
9-2	9813.6-9816.9	0.10	1,250		ss	Q?	2
9-3	9813.6-9816.8	1.10	101		ss	Q	1,4,5
9-5	9816.4-9817.7	0.08	396		ss	Q	1,4,5
10-1	9822.0-9823.5	--	457		ss	Q?	1,6
10-2	9823.1-9824.4	0.05	396	7,380	ss	Q?	1,6
10-3	9825.2-9827.2	<0.05	670		ss	Q+cc	6
10-5	9831.1-9831.9	<0.05	244		ss	Q?	6
10-7	9832.5-9834.2	--	518		ss	Q,cc,+ Anhy	3,4,6
11-2	9836.4-9837.4	<0.05	30	600	ss	Q?	5
11-3	9840.1-9840.7	<0.05	182		ss	Q	1,4,5
11-5	9840.9-9841.1	--	61		ss	Q	3,4,5
11-6	9841.5-9841.7	--	61		ss	Q	3,4,5
11-7	9841.9-9842.6	4.00	213	53	ss	Q	1,2,4,5,8

Table 3 (con't)

Core No.-Fracture No.	Core Depth (ft)	Width (W) (mm)	Length (L) (mm)	$\frac{L}{W}$	Rock Type	Vein Minerals	Notes
13-2	9861.0-9861.3	<0.05	91		ss	Q?	1
13-4	9861.8-9862.2	<0.05	122		ss	Q	2
13-8	9870.0-9880.3	0.08	3,139		ss	Q	1,4,5
13-9	9874.0-9876.9	--	884		ss	Q	3,4
14-19	9913.2-9915.5	<0.05	701		ss	Q	1
14-20	9915.1-9916.1	<0.05	30		ss	Q	3,4,5?
15-2	9918.9-9921.0	0.10	640	6,400	ss	Q	4?
15-8	9931.8-9932.7	<0.05	274		ss	Q?	1
15-10	9934.8-9934.9	--	30		ss	Q	4
15-11	9935.1-9935.3	0.08	61	762	ss	Q?	4?
15-12	9936.1-9936.9	0.51	274	537	ss	Q	4
15-13	9938.2-9939.5	<0.05	396		ss	Q	1

Abbreviations:

Q = quartz

cc = carbonate mineral

Anhy = anhydrite

-- = unknown

ss = sandstone

1 = en echelon, relay, or multiple fractures

2 = terminates within core

3 = terminates outside of core (true length unknown)

4 = fracture open or partly open in subsurface

5 = hydrocarbon fluorescence or mud gas in interval

6 = stress test interval

7 = possible natural fracture

8 = possibly associated with horizontal fractures

REFERENCES

CER Corporation, 1987, Observations and orientations of fractures induced through open hole stress tests: Report prepared for the Gas Research Institute, 30 p.

Dutton, S. P., 1987, Diagenesis and burial history of the Lower Cretaceous Travis Peak Formation, East Texas: The University of Texas at Austin, Bureau of Economic Geology Report of Investigations No. 164, 58 p.

Kulander, B. R., Barton, C. C., and Dean, S. L., 1979, The application of fractography to core and outcrop fracture investigations: Morgantown Energy Technology Center, report prepared for U. S. Department of Energy, METC/SP 79/3, 174 p.

Laubach, S. E., Baumgardner, R. W., Jr., and Meador, K. J., 1987, Analysis of natural fractures and borehole ellipticity, Travis Peak Formation, East Texas: The University of Texas at Austin, Bureau of Economic Geology, topical report prepared for Gas Research Institute under contract no. 5082-211-0708, 128 p.

Miall, A. D., 1985, Multiple-channel bedload rivers, in Flores, R. M., Ethridge, F. G., Miall, A. D., Galloway, W. E., and Fouch, T. D., eds., Recognition of fluvial depositional systems and their resource potential: Lecture Notes for Short Course No. 19, Society of Economic Paleontologists and Mineralogists, p. 83-100.

FIGURE CAPTIONS

Figures 1-4. Schematic representations of the vertical core profiles collected from the SFE No. 2 well. Cored intervals are correlated to the gamma-ray log as an aid in calibrating the log. Note that the core profile width is determined by a visual estimate of the sand content.

CORES 1-3

LOG DEPTH (FT) 0

GAMMA RAY 120 (API)

CORE PROFILE 100 % SAND 0

CORE DEPTH (FT)

DEPOSITIONAL ENVIRONMENT

8250

8250

8300

8300

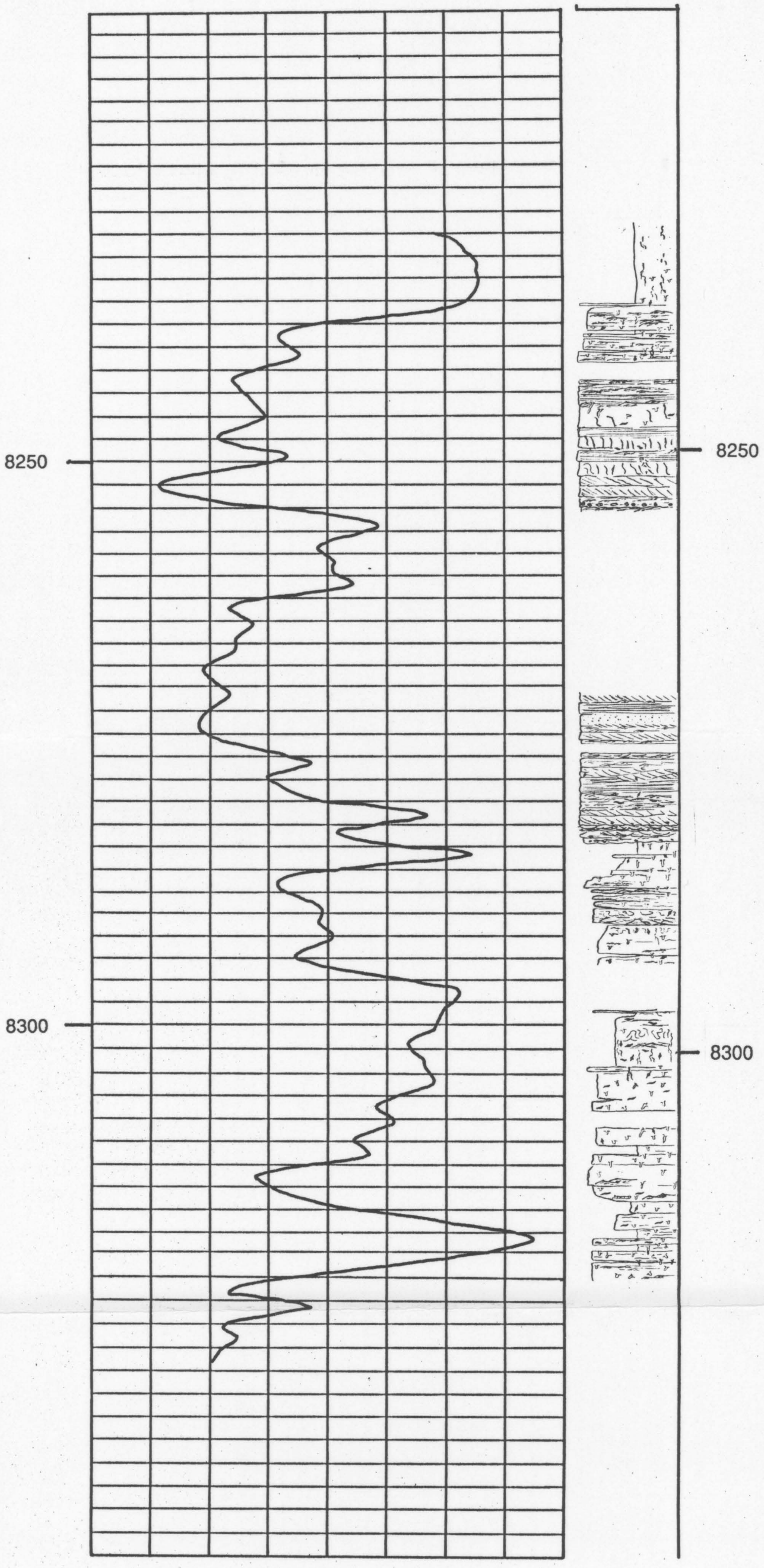

Floodplain

Channel

Floodplain Sandstone

Lacustrine

Floodplain

Floodplain Sandstone

Abandoned Channel

Channel

CORES 9-15

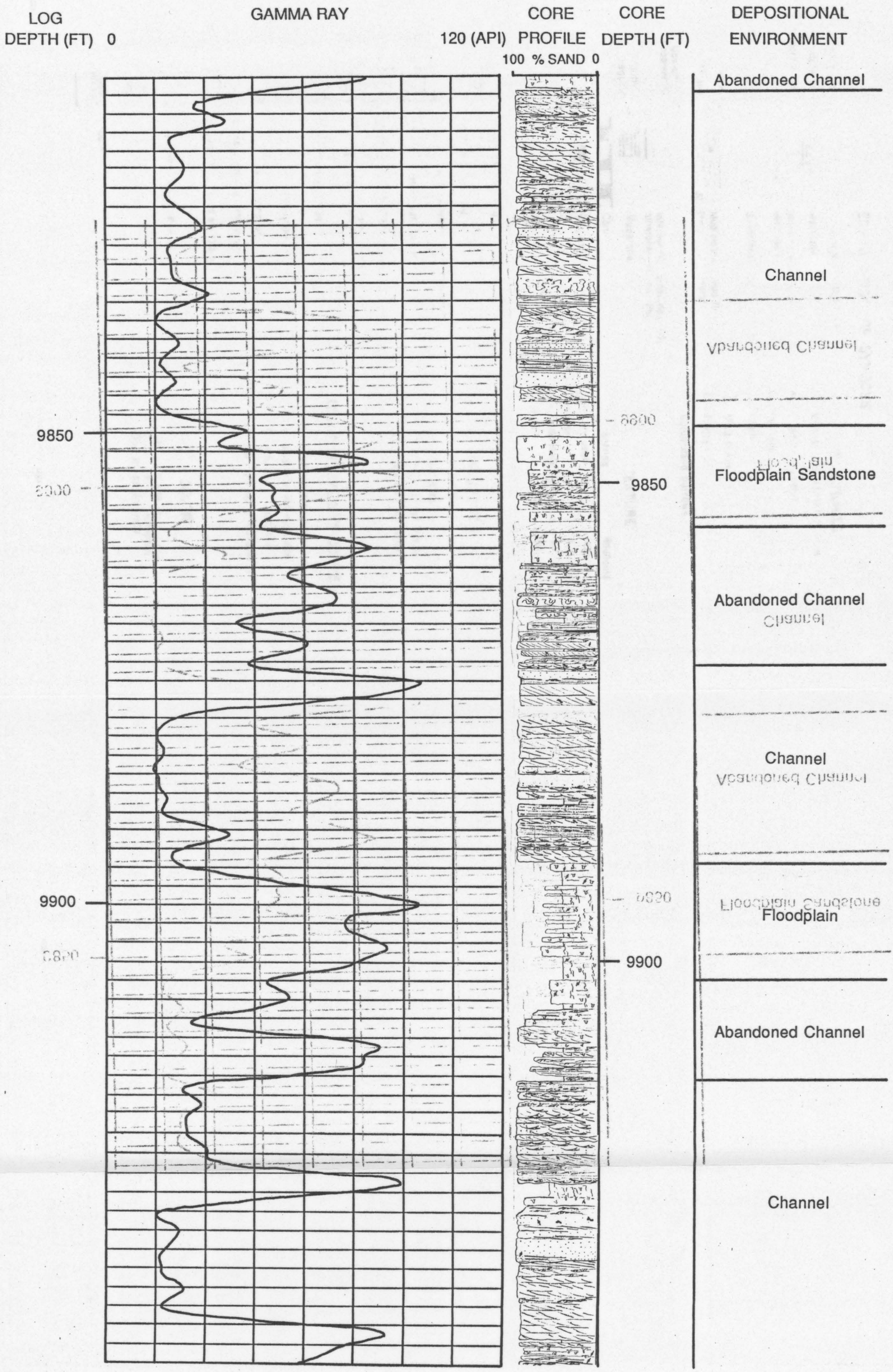
LOG
DEPTH (FT) 0
GAMMA RAY
120 (API)
CORE
PROFILE
100 % SAND 0
CORE
DEPTH (FT)
DEPOSITIONAL
ENVIRONMENT
Abandoned Channel
Channel
Floodplain Sandstone
Abandoned Channel
Channel
Floodplain
Abandoned Channel
Channel
9850
9900
9850
9900

CORES 6-8

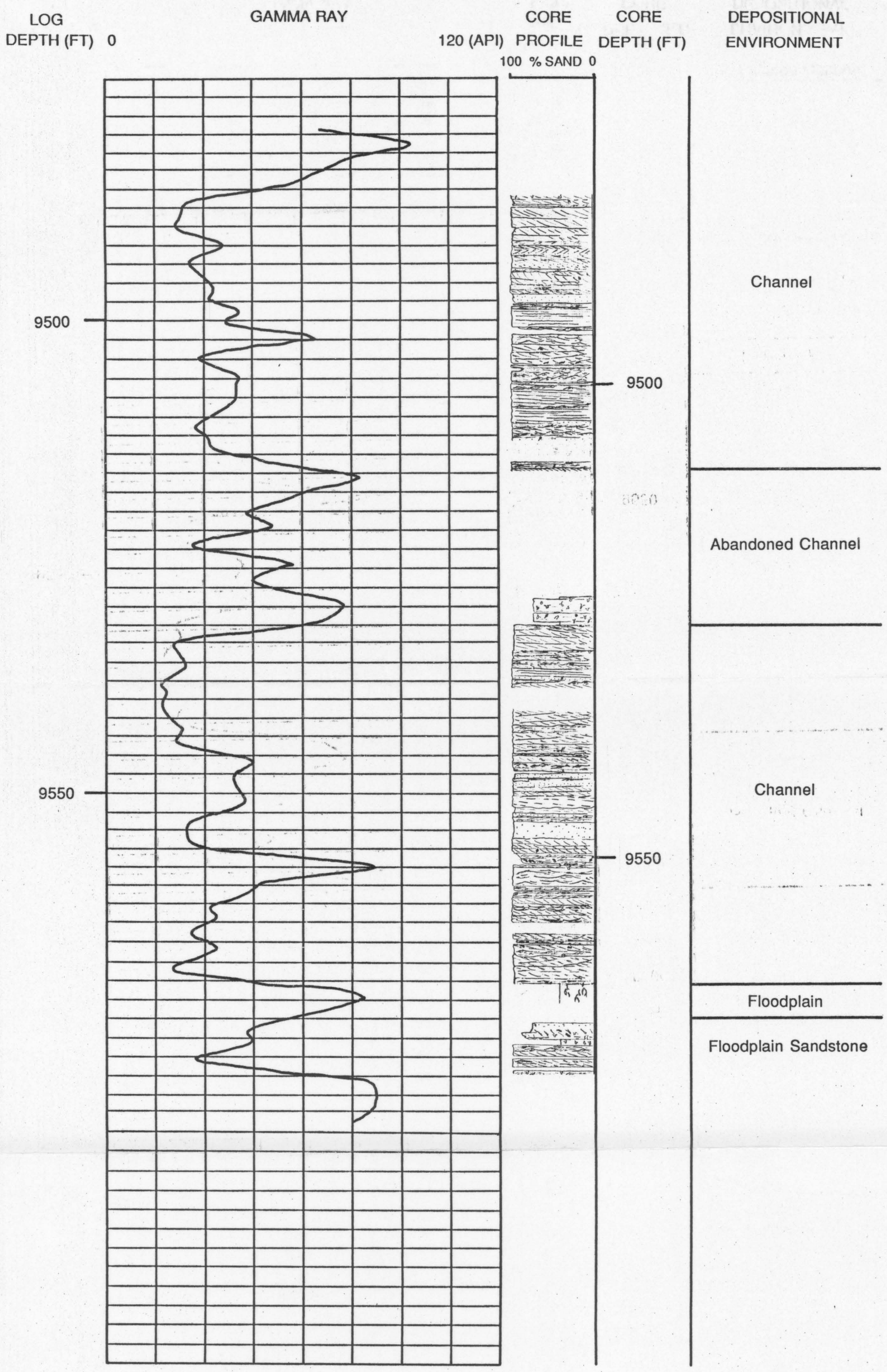
LOG
DEPTH (FT) 0
GAMMA RAY
120 (API)
CORE
PROFILE
100 % SAND 0
CORE
DEPTH (FT)
DEPOSITIONAL
ENVIRONMENT
9500
9550
9500
9550
Channel
Abandoned Channel
Channel
Floodplain
Floodplain Sandstone

CORES 4 & 5

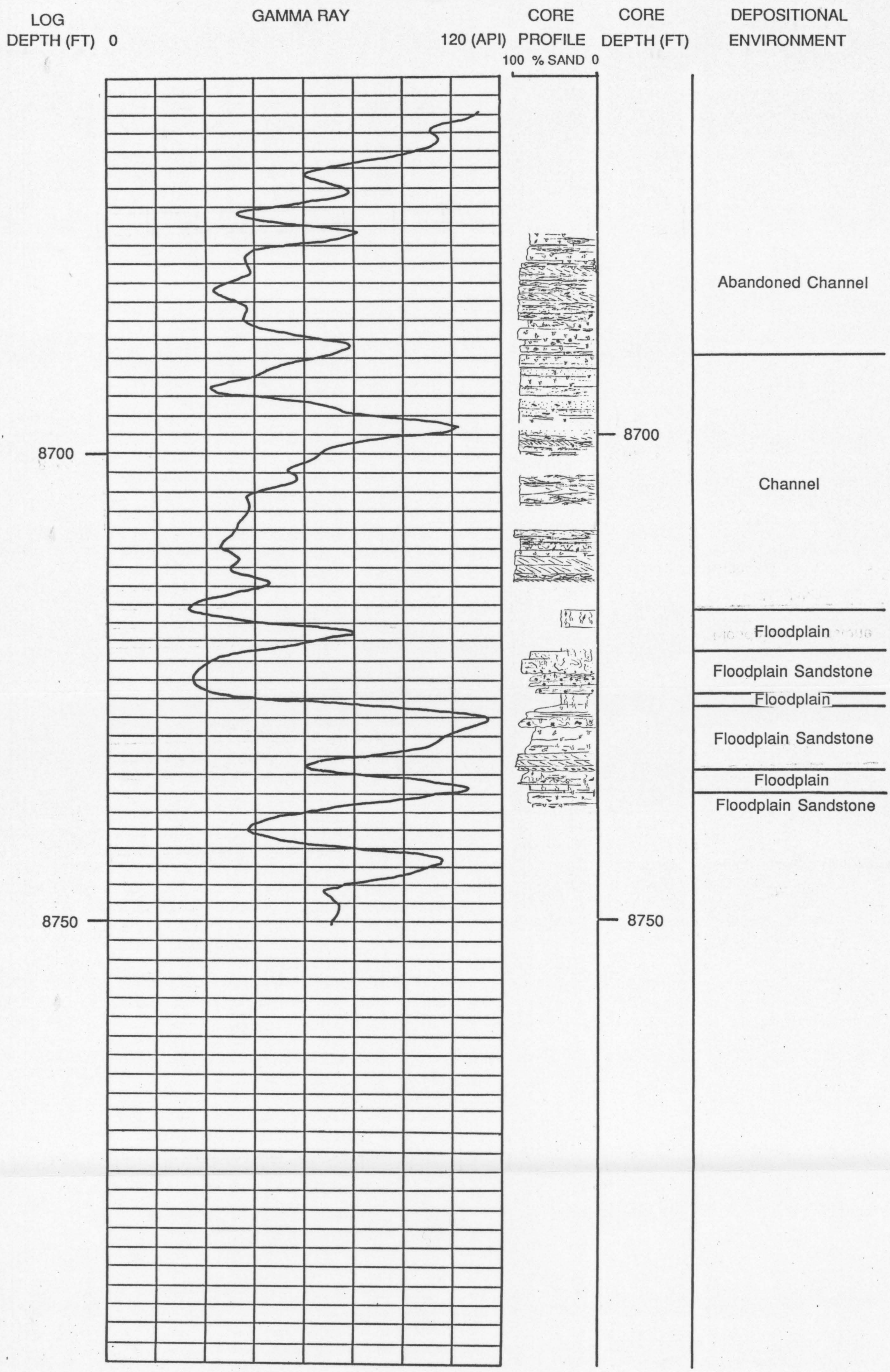
LOG
DEPTH (FT) 0
GAMMA RAY
120 (API)
CORE
PROFILE
100 % SAND 0
CORE
DEPTH (FT)
DEPOSITIONAL
ENVIRONMENT
8700
8700
8750
8750
Abandoned Channel
Channel
Floodplain
Floodplain Sandstone
Floodplain
Floodplain Sandstone
Floodplain
Floodplain Sandstone

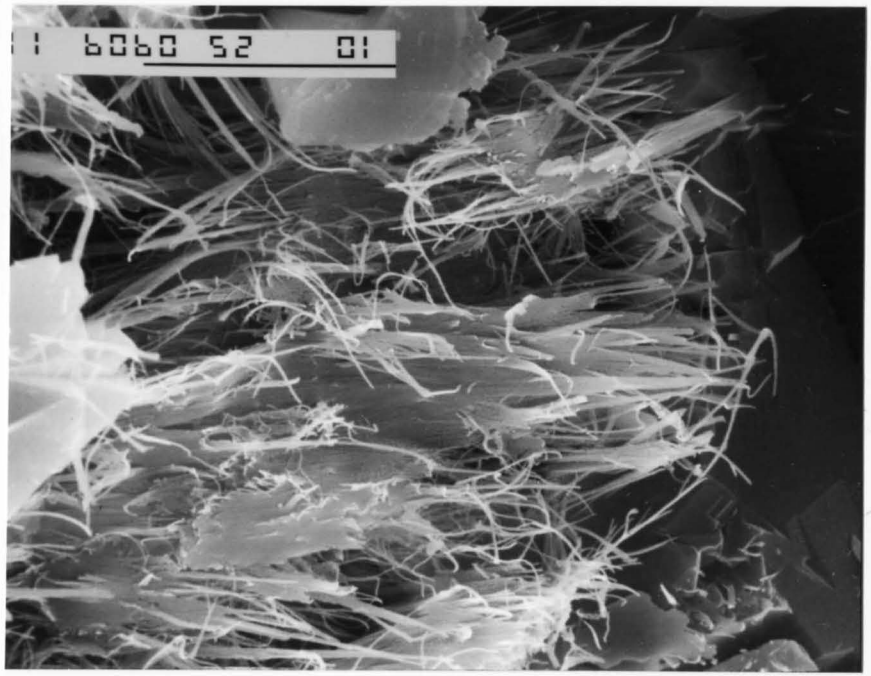
1 6060 52 01

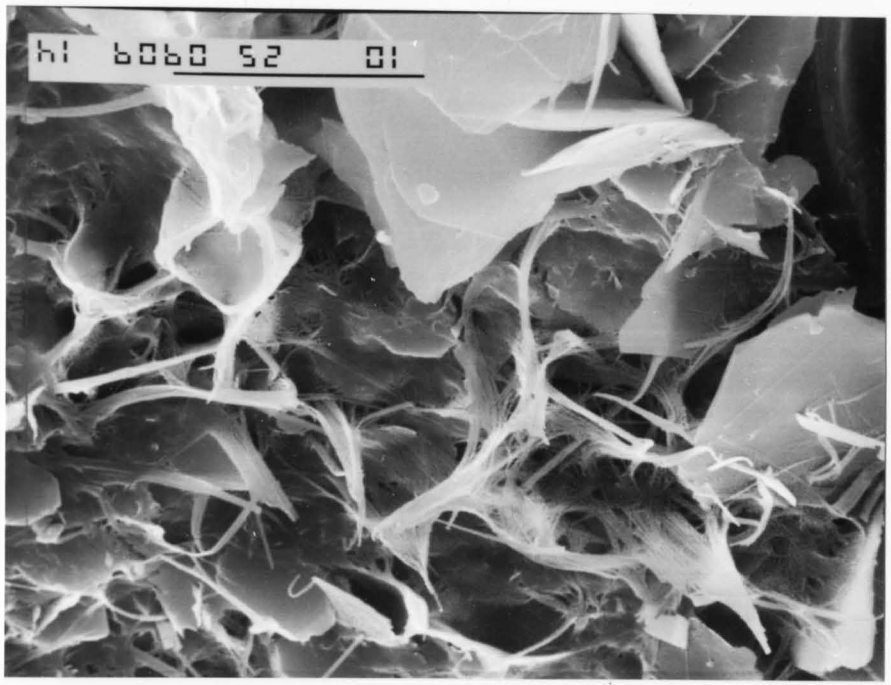
h1 6060 52 01

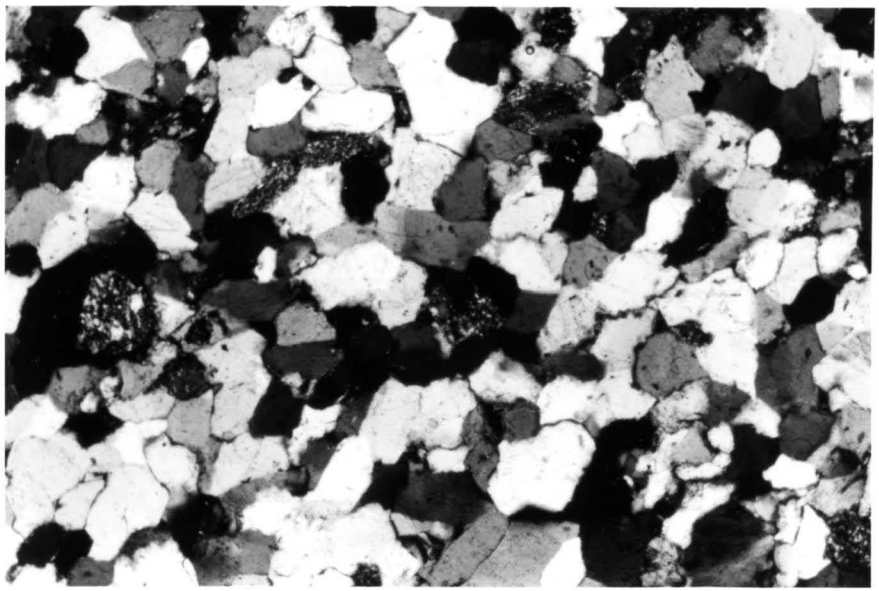

F I G U R E 5.

Photomicrograph of abundant quartz cement (27.5%) that completely occludes primary porosity, from a depth of 9,930.0 ft. Long dimension of photo is 2.6 mm. Crossed-polarized light.

F I G U R E 6.

SEM photograph of fracture-lining quartz facing open fracture. Depth is 9,872 ft. Bar length is 100 µm; magnification is 150x.

F I G U R E 7

SEM photograph of freeze-dried sample showing long, delicate thin fibers of illite. Depth is 9,816.8 ft. Bar length is 10 µm; magnification is 3500x.

F I G U R E 8

SEM photograph of air-dried sample showing matted and collapsed illite fibers. Sample depth is 9,816.8 ft, from the same plug as the sample in figure 7. Bar length is 10 µm; magnification is 3500x.

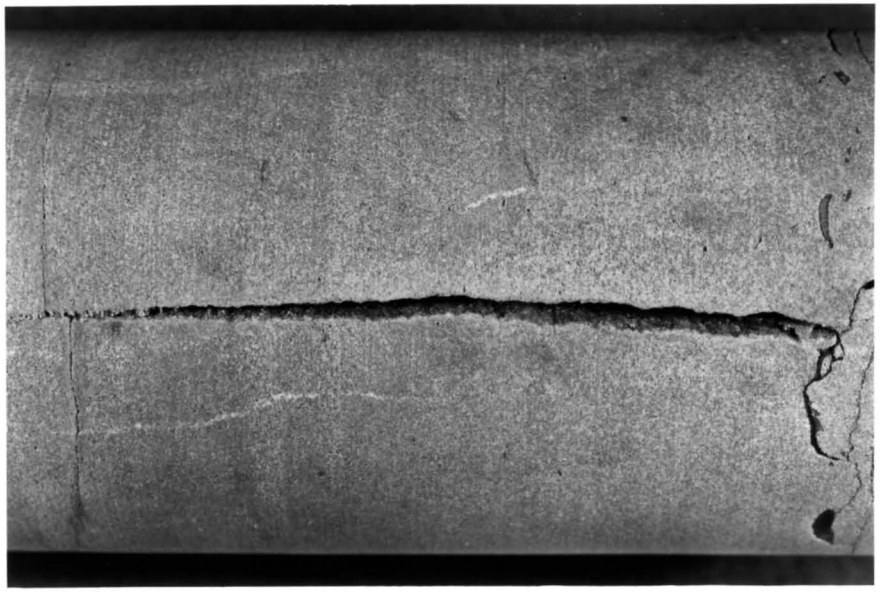

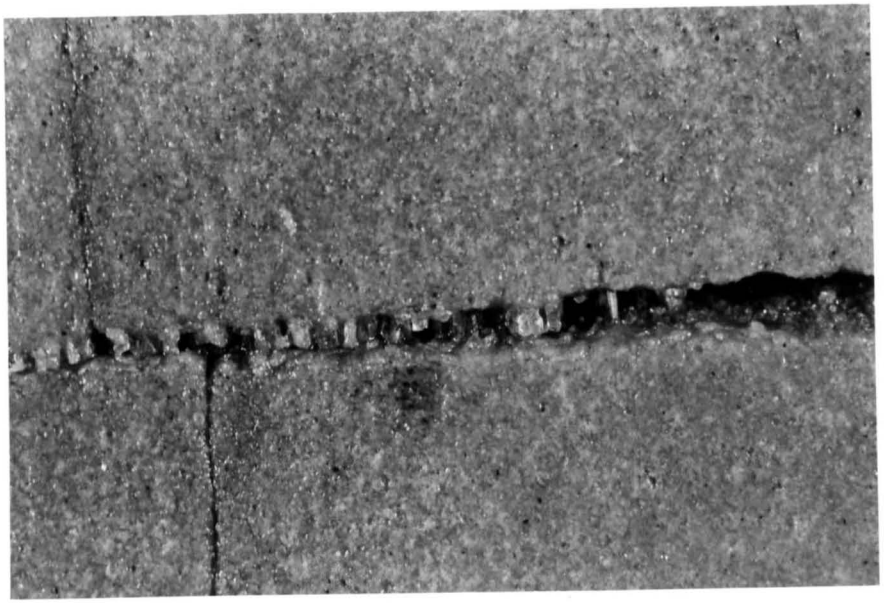

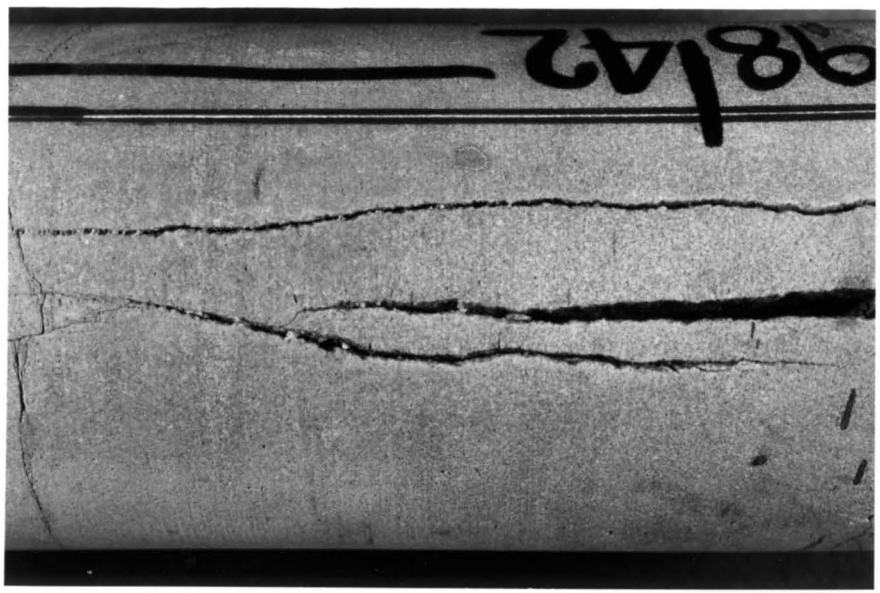
9814

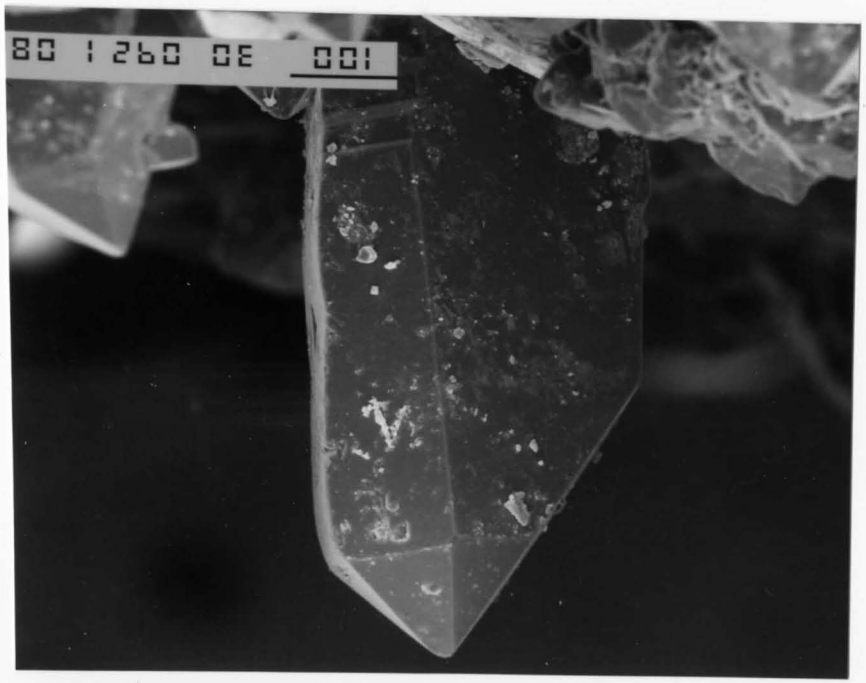
08 1260 30 001

Figure 9. Four views of the natural open fracture at 9,842 ft.

F I G U R E 9a.

Single fracture with a 4 mm aperture. Upper fracture termination is blunt. Long dimension of photo is 12 cm.

F I G U R E 9b.

Close-up view of the lower, tapering termination of the fracture. Note the acicular quartz crystals lining the main fracture and the horizontal fractures emanating from the main vertical fracture. Long dimension of photo is 3.5 cm.

F I G U R E 9c.

View of the same fracture on the other side of the core. Multiple fracture traces are evident. Long dimension of photo is 12 cm.

F I G U R E 9d.

View of quartz on the fracture face. Long dimension of photo is 5 cm.

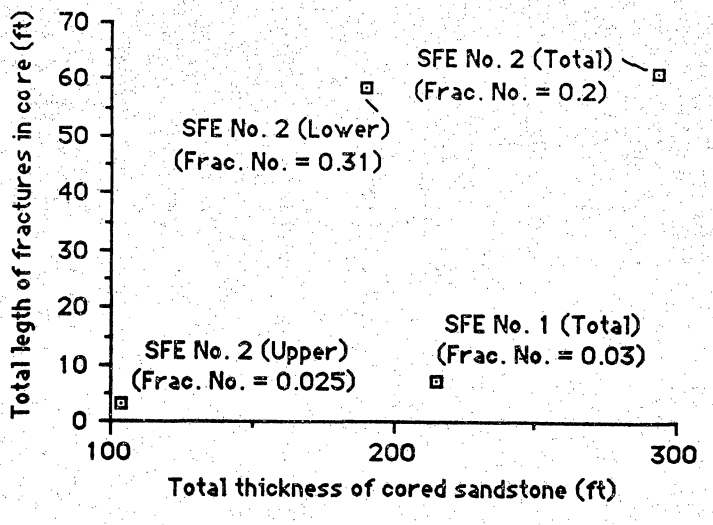

Figure 10. Fracture number, defined as total fracture length in core normalized to sandstone thickness in core, for the upper (8,000 to 9,000 ft) and lower (9,000 to 10,000 ft) Travis Peak at SFE No. 2 and the Holditch Howell No. 5 (SFE No. 1) - Harrison County, Texas.

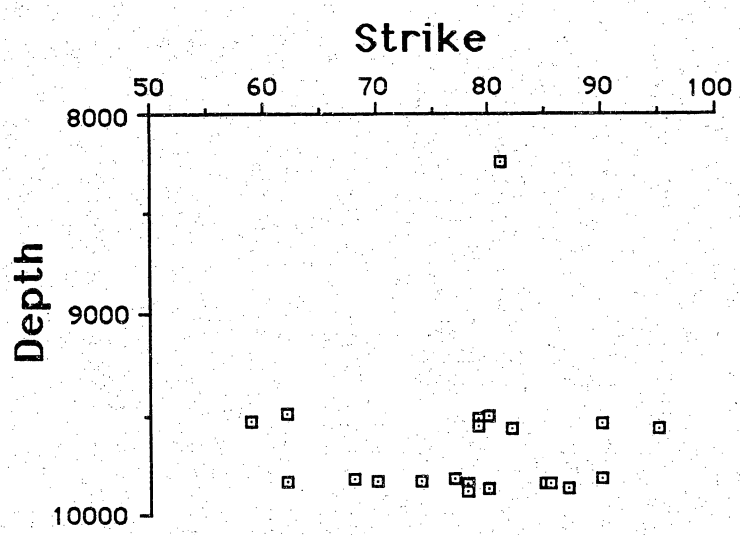

Figure 11. Natural fracture strike versus depth (ft). Preliminary results based on correlation of natural fractures in core to BHTV images.

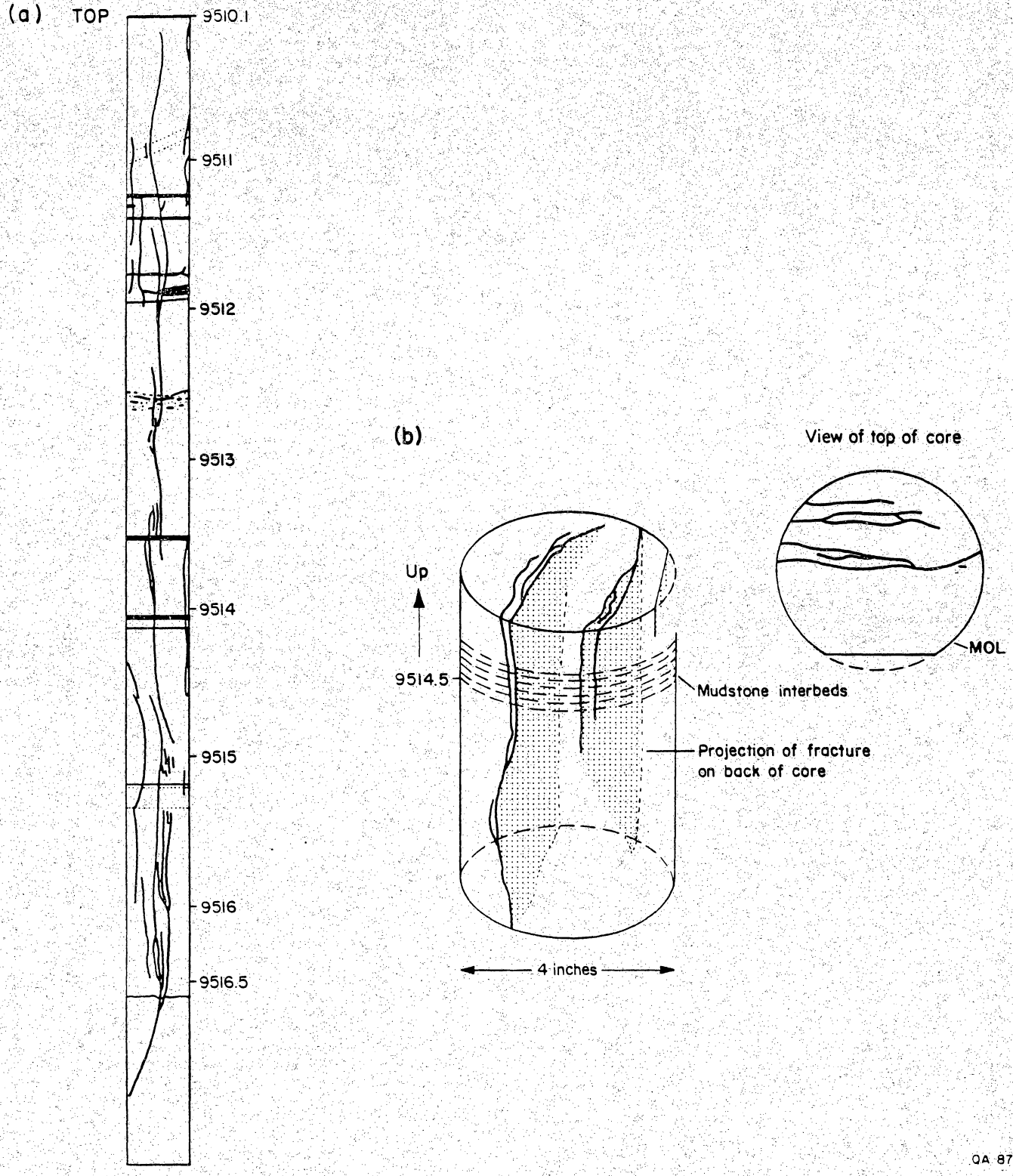

Figure 12. Field sketch of the hydraulic fracture induced by open-hole stress test 2, core 7. (a) Overall sketch of the fractured interval showing multiple fracture strands. The fracture strands occur in very fine grained sandstone, occasionally gradational to muddy sandstone, with local thin beds of dark gray shale and shale rip-up clasts. (b) Detail of part of the stress test fracture set, showing the three dimensional relation of individual fracture planes. Inset shows map of the top of the core in this interval.